Invited Paper

Development and application of noninvasive optical topography

Tsuyoshi Yamamoto[1][1], Atsushi Maki[1], Yuichi Yamashita[1], Hiroshi Yoshizawa[2], Makoto Iwata[2], Eiju Watanabe[3], Yukari Tanikawa[4], Yukio Yamada[4], and Hideaki Koizumi[1]

[1] Advanced Research Laboratory, Hatoyama, Saitama 350-0395, Japan
[2] Tokyo Women's Medical University, 8-1 Kawada, Shinjuku, Tokyo, 162-8666, Japan
[3] Tokyo Metropolitan Police Hospital, 2-10-41, Fujimi, Chiyoda, Tokyo, 102-8161, Japan
[4] Mechanical Engineering Laboratory, 1-2 Namiki, Tsukuba, Ibaraki 305-8564, Japan

ABSTRACT

Optical topography (OT) is a method for visualizing brain functions noninvasively. In an OT measurement system, near-infrared light, to which living tissue is highly permeable, is irradiated from the scalp of the subject, and the scattered light reflected from the cerebral cortex is detected elsewhere on the scalp. The spatio-temporal blood volume change in the cortex is visualized based on the signal detected using two-dimensionally arranged optodes. The measurement imposes few constraints on the subject, either physically or mentally, thus the subject is in a natural and relaxed condition during measurement. Here, we describe out OT system, then report on an experiment to evaluate the system using a phantom. We found that OT can accurately locate the activated region in the cortex. Also, as an example of a clinical application of OT, we used our system to measure the language function, demonstrating the system's ability to measure the activity of Broca's area.

Key Words: optical topography, brain function, blood-volume, phantom, and language function

1. INTRODUCTION

The systematic clarification of human brain functions will lead to wide application in fields such as psychology, information engineering, and educational engineering, as well as in the field of clinical medicine. For this reason, various measurement systems have been developed. The electroencephalogram which Berger invented in 1929 measures the electric current induced by the activity of nerve cells in the brain [1]. This method, known as EEG, is used in clinical medicine and in clarifying brain functions. Other than EEG, several noninvasive measurement systems - MEG (magnetoencephalography), PET (positron emission computed tomography), and fMRI (functional magnetic resonance imaging) - have been proposed [2-4]. In these measurement systems, the subject is highly restrained. The subject is kept with in a narrow space and cannot move during the examination, thus it is difficult for the subject to relax.

The measurement of brain functions using near-infrared spectroscopy (NIRS) imposes little restraint on the subject. In this method, near-infrared light, to which living tissue is highly permeable, is irradiated from the scalp of the subject and the light scattered in the cerebral cortex is detected on the scalp [5-7]. This method measures the change in the blood-volume associated with brain activation. When brain nerve cells are activated, blood-volume increases to supply more oxygen to these cells, and this increase is detected through the change in absorption of the light due to the increased hemoglobin (Hb) content.

Based on the NIRS method, the authors developed optical topography (OT), a method in which blood-volume changes are measured at multiple points on the scalp for a subject. In OT, the signals are detected by two-dimensionally arranged optodes, and the spatio-temporal activity of the brain is visualized from these signals [8-11].

In this paper, we explain the principles of measuring brain functions by NIRS and describe the 24-

[1] Correspondence: TEL:+81-492-96-6111, E-mail:tymt@harl.hitachi.co.jp, http://hatoyama.hitachi.co.jp.

In *Optical Sensing, Imaging, and Manipulation for Biological and Biomedical Applications*, Robert R. Alfano, Ping-Pei Ho, Arthur E. T. Chiou, Editors, Proceedings of SPIE Vol. 4082 (2000) • 0277-786X/00/$15.00

channel OT measurement system developed by our group. After that, we report on our evaluation of the location accuracy of OT, which was done using a phantom. It is difficult to directly evaluate with high accuracy the position inside the actual brain where the blood volume changes. The phantom was used to simulate the light scattering characteristics of living tissue and the blood-volume change associated with the brain activation. Finally, a clinical application of OT is described. The brain activity associated with the language function was measured with our OT system, and it was clearly shown that the blood-volume increased in Broca's area.

2. METHODS

2-1 Principle of OT

Figure 1 shows the method used to measure blood-volume change in the cortex. The near-infrared light enables high optical permeability through the various types of tissue, but it is strongly scattered by these tissues. Thus, only part of the light is transmitted through the skull and reflected from the cerebral cortex at about 15 mm below the scalp. The reflected light reaches the scalp again at a distance of about 30 mm from the illuminated point. The Hb in the blood absorbs the near-infrared light. If the blood-volume, and thus the absorption coefficient, increases in the cortex because of brain activation during the stimulation period, the intensity of the reflected light decreases. Therefore, the difference between reflected-light intensities R and R^s, obtained before and after the stimulation, respectively (Fig. 1), provides information on the blood-volume change in the cortex.

In the actual measurement (Fig. 2), two 0.5-mW-output continuous wave (CW) lasers with a wavelength of 780 nm or 830 nm are used as light sources to measure the change in the concentration of the oxy-Hb and deoxy-Hb. The oscillators operate at different frequencies on the order of 1 kHz to modulate the diode output power. The outputs from the diodes are mixed by an optical fiber coupler, and illuminated onto the scalp. After the reflected light passes through the human tissue it is picked up by an optical fiber. The photodiode then converts the reflected light into an electrical signal and sends the signal to two lock-in amplifiers. Each lock-in amplifier, which refers to the modulation frequency of each light source, separates the reflected light into one of the two original wavelengths (780 nm or 830 nm). The reflected intensity $R(\lambda,t)$ for the wavelength λ (780 nm or 830 nm), and measurement time t is obtained and sent to the analog/digital (A/D) converter. A personal computer analyzes the reflected intensity.

When the subject is at rest (before brain activation), $R(\lambda,t)$ satisfies

$$-\ln[R(\lambda,t)]=\varepsilon_{oxy}(\lambda)C_{oxy}(t)d+\varepsilon_{deoxy}(\lambda)C_{deoxy}(t)d+sc(\lambda), \quad (1)$$

where $\varepsilon_{oxy}(\lambda)$ and $\varepsilon_{deoxy}(\lambda)$ are the molar absorption coefficients of oxy-and deoxy-Hb, respectively. C_{oxy} and C_{deoxy} are the concentrations of oxy- and deoxy- Hb, d is the effective path length in the tissue, and $sc(\lambda)$ is the attenuation due to the scattering in the tissue. In the same way, when the subject is activated by the stimulation, the reflected intensity $R^s(\lambda,t)$ satisfies

$$-\ln[R^s(\lambda,t)]=\varepsilon_{oxy}(\lambda)C^s_{oxy}(t)d+\varepsilon_{deoxy}(\lambda)C^s_{deoxy}(t)d+sc(\lambda), \quad (2)$$

where the superscript "s" denotes stimulation. By subtracting equation (1) from equation (2), we obtain

$$-\ln[R^s(\lambda,t)/R(\lambda,t)]=\varepsilon_{oxy}(\lambda)[C^s_{oxy}(t)-C_{oxy}(t)]d+\varepsilon_{deoxy}(\lambda)[C^s_{deoxy}(t)-C_{deoxy}(t)]d. \quad (3)$$

We rewrite the right-hand side of equation (3) as

$$-\ln[R^s(\lambda,t)/R(\lambda,t)]=\varepsilon_{oxy}(\lambda)\Delta C_{oxy}(t)+\varepsilon_{deoxy}(\lambda)\Delta C^s_{deoxy}(t), \quad (4)$$

where

$$\Delta C^s_{oxy}(t)=[C^s_{oxy}(t)-C_{oxy}(t)]d, \quad (5)$$

$$\Delta C^{s}_{deoxy}(t)=[C^{s}_{deoxy}(t)- C_{deoxy}(t)]d, \quad (6)$$

respectively, because the value of d in the tissue is difficult to obtain at present. The ratio of the reflected intensities in the left-hand side of equation (4) is measured at each wavelength (780 nm and 830 nm), and the concentration changes of the oxy-Hb and deoxy-Hb are obtained. The concentration change of the total-Hb is the sum of these.

To obtain a topographic image of the blood-volume change, an array of optodes that act as light sources (incident positions) and optodes that act as detectors (detection positions) are placed on the subject's scalp. Figure 3 shows the 24-channel measurement system. 16 light sources (eight sources for each wavelength of 780 nm and 830 nm) and eight avalanche photodiodes (Hamamatsu C5460-01) are employed. For the light illumination on the scalp and to pick up the transmitted light, optical fibers with a 1-mm cladding diameter are attached to the scalp to eliminate interference from hair. These optodes that make up each source-detector pair are separated by 30 mm. The sensitivity to the blood-volume change is highest at the middle point of each optode pair, so the middle points are used as measurement points [12]. In the Fig. 3, there are 24 measurement points at the middle of the optode pairs. The minimum distance between measurement points is 21 mm, and the octagonal measurement area, surrounded by these measurement points, is 90 × 90 mm. The blood-volume changes at these 24 measurement points are estimated, then a topographic image of the changes is obtained by spline interpolation.

2-2 Phantom for OT

Here, we have developed a phantom that can be used to simulate the brain activation measured by OT. For clinical application of the OT, location accuracy of the topographic image is critical, but the location of the blood-volume change inside the cerebral cortex is difficult to detect accurately. The blood-volume increase in the cortex is analogous to an increase in the absorption coefficient within a scattering medium. Our phantom simulates the light scattering characteristics of the living tissue.

The phantom is made of epoxy resin (Buehler Corp.) containing the powdered titanium-oxide (TiO_2, KA30-K: Titan Kogyo Corp.)[13], and it consists of the body and inserts (Fig. 4). The size of the body is 200 × 200 × 40 mm to model the adult head size. The surface area of the body is five times the measurement area of the 24-channel system in Fig. 3 to avoid the effects of light reflection at the boundary. The height of the body is more than double the depth from the scalp to the cortex (15 mm). The scattering and absorption coefficients of this phantom, estimated by the time-resolved measurement method [14], were respectively 0.5 mm^{-1} and 0.0 mm^{-1} at the 830-nm wavelength.

To simulate brain activation, the absorption coefficient inside the phantom should be variable. A 10-mm-diameter hole was drilled in the center of the phantom, and inserts to be placed inside of the phantom were prepared. The structure of the inserts (A) and (B) in Fig. 4 are homogeneous and heterogeneous, respectively. The optical properties of insert (A) and sections (I) and (III) of insert (B) are the same as those of the body. On the other hand, section (II) of insert (B) contains a greenish brown light absorber. This light absorber has absorption in the NIR region and its absorption coefficient is 0.025 mm^{-1}. In Figs. 5(a) and (b), inserts (A) and (B), respectively, are placed inside the body of the phantom. The absorber is located near the center of the phantom and simulated the blood-volume (absorption coefficient) change in the cerebral cortex.

The measurement system we used to evaluate our phantom is shown in Fig. 6. The optodes were arranged on the phantom. Eight laser light sources (wavelength: 830 nm) were modulated at different frequencies (1 to 10 kHz), and were coupled to the eight optodes used for illumination. Eight optodes to detect the transmitted light were connected to avalanche photodiodes. The outputs from the photodiodes were sent to lock-in-amplifiers that separated the transmitted light intensity into the 24 measurement points. The data were processed with a computer.

To obtain a topographic image of the absorber in the phantom, the absorbance change ΔA at each of the 24 measurements point is given as,

$$\Delta A = - \ln (R^{s}/ R) \quad (7),$$

where, R^s and R denote the reflected intensities with the light absorber and without the absorber in the phantom, respectively. The distribution of ΔA inside the measurement area was estimated and a topographic image of the absorber in the phantom was obtained.

2-3 Language function measurement

The language function is a brain function peculiar to humans. There is powerful need for a method of measuring the language function for both basic research and clinical medicine purpose. In our language function measurement, the subject was shown a picture of an object to activate the language function. The subject wrote the word for the object and an inspector objectively checked and evaluated the activation of the subject's language function. Measurement with a conventional brain function measuring system is difficult, because the head of the subject moved during the test and this movement caused signal noise.

Since the optical fibers used to irradiate and detect reflected light in OT are attached to the subject's scalp, there is little noise during the measurement even if the subject moves a little. Thus, the subject is likely to feel more natural and relaxed, compared, for example, to when being examined by MRI during which immobility and an uncomfortable posture is required. For realistic language-function measurement, an OT system may therefore be indispensable.

In this experiment, language functions were activated by a writing task rather than a speaking task because the load is generally considered to be higher for a writing task[15]. There are two language function areas in the cortex: Broca's area in the frontal lobe, and Wernicke's area in the temporal lobe. The subject was a 27-year-old right-handed healthy male volunteer. Almost all (99 %) right-handed people have language function territory fields on the left hemisphere sinciput, so the measurement area was arranged on the subject's left hemisphere sinciput. Informed consent was obtained from the subject before the investigation. The subject was awake and sitting relaxed in a chair. No special room was required for this experiment, which would not be the case for PET or fMRI. The location of the subject's language function area was estimated by anatomic MRI and with the neuronavigator [16]. The task sequence for this experiment is shown in Fig. 7. The subject was shown a card with a picture of an object for 3 seconds(In Fig. 7, a picture of a knife is shown). During the 3 seconds, the subject wrote down the name of the object in Japanese "*kana*" which is a phonetic syllabary. The task was repeated 30 times so the total stimulation period was 90 seconds. As a control task, the subject was shown a figure with no meaning, which he was required to draw. The shape vaguely resembled Japanese "*kana*", and would require a similar drawing motion for 3 seconds. Sample figures for this experiment are shown on both sides of the picture of the knife in Fig. 7. During the writing and control tasks, the motor area located in the frontal lobe was activated, because the subject moved his arm and hand when writing letters and drawing figures. Therefore, the activation of the motor area was eliminated by subtracting the signal intensities during the control task from the signal intensities during the writing task. In the same way, the signal from the visual cortex could be removed. The control task was performed as pre-simulation for a total of 60 seconds and as post-stimulation for a total of 70 seconds. The subject rested for 30 seconds between post-stimulation and pre-stimulation for the next series of the task.

3. RESULTS AND DISCUSSION

3-1 Location accuracy

Figure 8 shows topographic images of ΔA and the relative locations of the optodes on the phantom and the absorbers in the phantom. In Fig. 8(a), the absorber was set midway between two optodes, where ΔA sensitivity was the highest. On the other hand, in Figs. 8(b) and (c), the absorbers were placed below an optode and at the center of four optodes, respectively. These figures show that the location of the absorber on the topographic image was consistent with the actual location inside the phantom within a 3-mm margin of error. This value is less than the interval between the measurement points (21 mm). This value is also lower than the size of the visual cortex (more than 20 × 20 mm) and of the motor area (more than 10 × 10 mm) [17]. Therefore, these results demonstrate that the OT system can be used to identify the area of brain activation.

However, the full width at half maximum of each ΔA distribution was more than 20 mm. This is more than twice the diameter of the absorber inside the phantom. Thus, the spatial resolution of the topographic image needs to be improved.

3-2 Language function measurement

Figure 9 shows a spatial map of the change in total-Hb obtained during the writing task and MRI of the subject. To obtain this static topographic image, we averaged the change in Hb-concentration during the writing task, compared to before and after at each channel position. Furthermore, the z-value of the total-Hb concentration change at each measurement point was obtained. Among the 24 measurement points, the z-value at channel 9 was the largest, and this channel corresponded to the Broca's area of the subject as indicated by the MRI. Figure 10 shows the temporal change in the oxy-Hb, deoxy-Hb, and total-Hb concentrations for channels 9 and 1. A hemodynamic response was observed approximately 30 seconds after the writing task started and the peak response occurred at about 60 seconds after the start. In the region showing the highest activity there was an increase in oxy-Hb and total-Hb with a decrease in deoxy-Hb. This is consistent with increased metabolic demand. On the other hand, in the outer region of Broca's area, for example at the measuring point of channel 1, the oxy-Hb concentration and the total-Hb concentration decreased 30 seconds after the writing task started.

4. CONCLUSION

Optical topography offers clear advantages for noninvasive brain function measurement compared to other methods, we have developed a 24-channel OT system. To evaluate the topographic imaging of our system, we created a phantom to simulate light scattering by the live tissue and the blood volume change in the cortex. The topographic images identified the position of the light absorber in the phantom with an accuracy of 3 mm. A potential application of optical topography is language function measurement, and in doing this we observed increased blood-volume in Brocs's area during a writing task.

REFERENCES

1. H. Berger, "Über das Electrenkephalogramm des Menschen". Archiv für Psychiatrie **87**, 527-570(1929).
2. D. Cohen, "Magnetic field around the torso: Production by electrical activity of the human torso". Science **156**, 652-654(1967).
3. M. E. Raichle, "Measurement of local cerebral blood flow and metabolism in man with positron emission tomography". Fed. Proc. **40**, 2331-2334(1981).
4. S. Ogawa, T. -M. Lee, A.S. Nayak and P. Glynn, "Oxygenation-sensitivity contrast in magnetic resonance image of rodent brain at high magnetic fields". Magn. Reson. Med. **14**, 68-78(1990).
5. F. F. Jöbsis, "Non-invasive infrared monitoring of cerebral and myocardial oxygen sufficiency and circulatory parameters". Science **198**, 1264-1267(1977).
6. M. Cope and D. T. Delpy, "A system for long term measurement of cerebral blood and tissue oxygenation in new born infants by near-infrared spectroscopy". Med. Biol. Engl. Comp. **32**, 1457-1467(1988).
7. T. Kato, A. Kameim S. Takashima and T. Ozaki, "Human visual cortical function during photic stimulation monitoring by means of near-infrared spectroscopy". J. Cereb. Blood Flow Metab. **13**, 516-520(1993).
8. A. Maki, Y. Yamashita, Y. Ito, E. Watanabe and H. Koizumi, "Spatial and temporal analysis of human motor activity using noninvasive NIR topography". Med. Phys. **22**, 1997-2005(1995).
9. Y. Yamashita, A. Maki, Y. Ito, E. Watanabe, Y. Mayanagi and H. Koizumi, "Noninvasive near-infrared topography of human brain activity using intensity modulation spectroscopy". Opt. Eng. **35**, 1046-1049(1996).
10. E. Watanabe, Y. Yamashita, A. Maki, Y. Ito and H. Koizumi, "Non-invasive functional mapping with multi-channel near-infrared spectroscopic topography in humans". Neurosci. Lett. **205**, 41-44(1996).
11. H. Koizumi, Y. Yamashita, A. Maki, T. Yamamoto, Y. Ito H. Itagaki and R. Kennan, "Higher-order brain function analysis by trans-cranial dynamic near-infrared spectroscopy imaging". J. of Biomed.

Opt. 4, 403-413(1999).
12. P. W. McCormich, M. Stewart, G. Lewis, M. Dujovny and J. I. Ausman: "Intracerebral penetration of infrared light", J. Neurosurg., **76**, 315-318(1992).
13. M. Firbank, M. Hiraoka and D. T. Delpy: "Development of a stable and reproducible tissue equivalent phantom for use in infrared spectroscopy and imaging", Proceeding of SPIE, **1888**, 264-270(1993).
14. G. Zaccanti, P. Bruscaglioni, A. Ismaelli, L. Carraresi, M. Gurioli and Q. Wei: "Transmission of a pulsed thin light beam through thick turbid media: experimental results", Appl. Opt., **31**, 2141-2147(1992).
15. T. Yamamoto, Y. Yamashita, H. Yoshizawa, A. Maki, M. Iwata, E. Watanabe and H. Koizumi, "Non-invasive measurement of language function by using optical topography", Proc. of SPIE **3597**, 250-237(1999).
16. E. Watanabe, T. Watanabe, S. Manaka, Y. Mayanagi and K. Takakura, "Three-dimensional digitizer (neuronavigator): New equipment for computed tomography-guided stereotaxic surgery", Surg. Neurol. **27**, 543-547(1987).
17. J. Talairach,. P. Tournoux, "Co-planar stereotactic atlas of the human brain", Thieme Press, New York (1988).

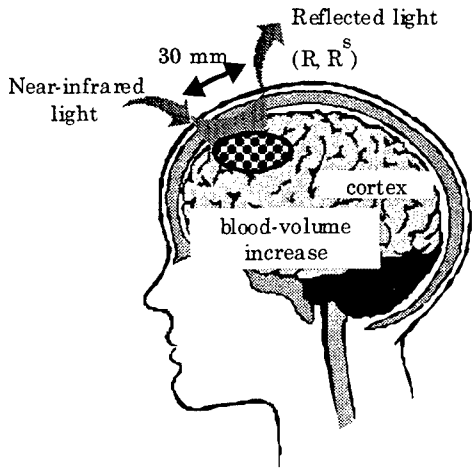

Figure 1 Method used to measure the blood-volume change in the cortex.

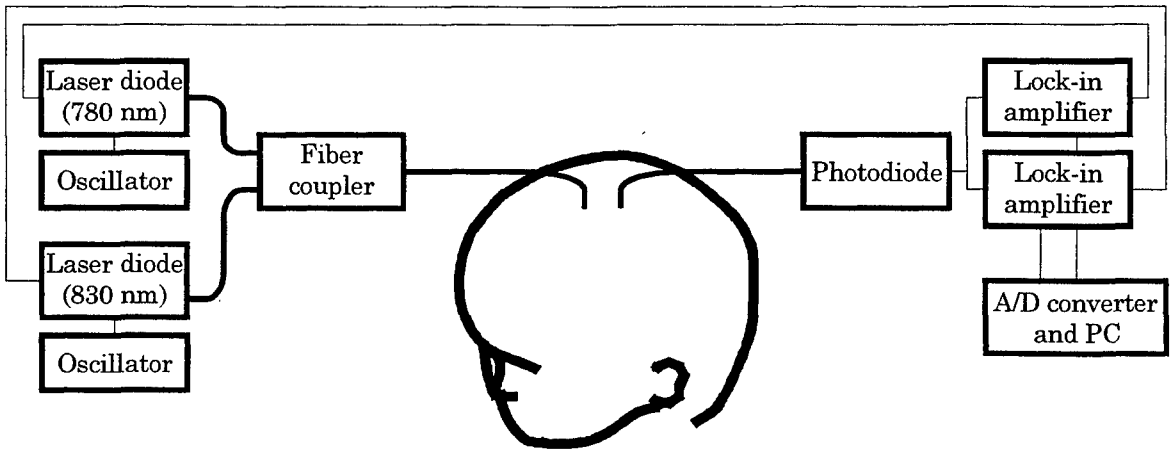

Figure 2 Method used to measure the change in concentration of the oxy-Hb and deoxy-Hb by NIR spectroscopy.

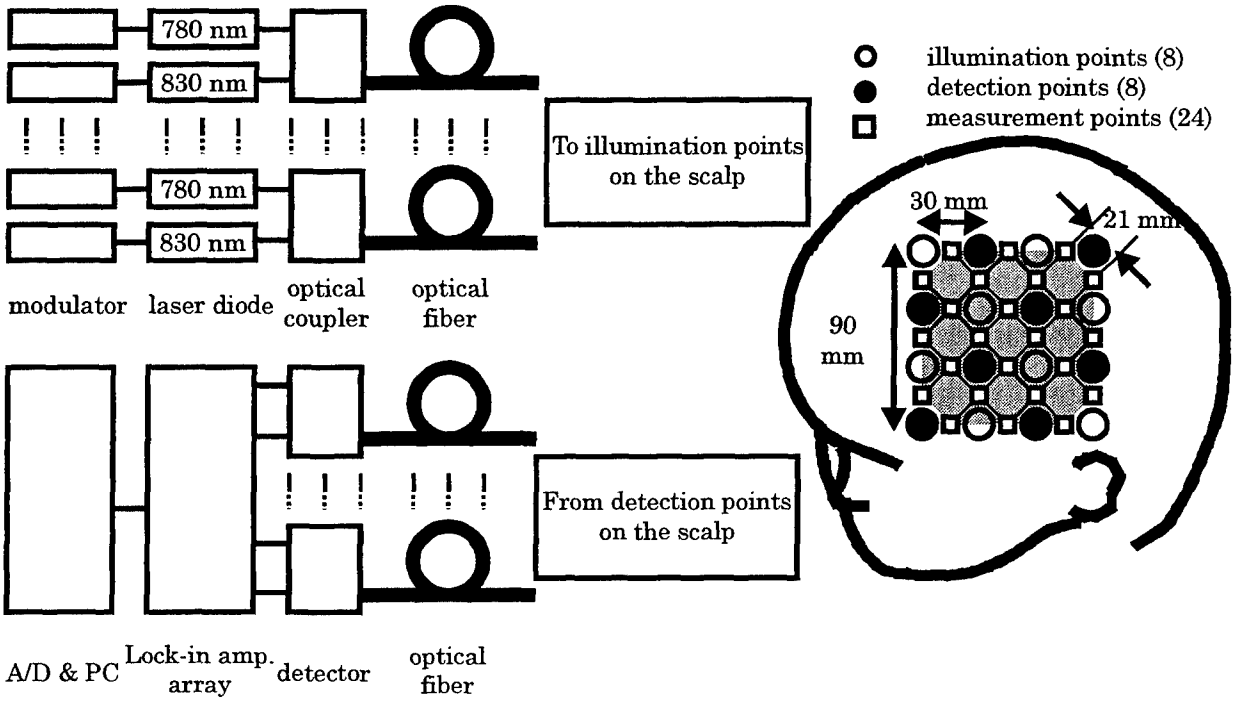

Figure 3 The 24-channel measurement OT system.

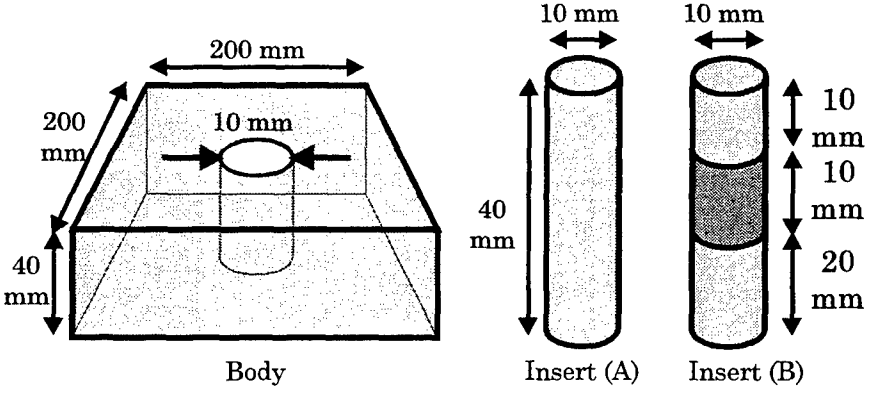

Figure 4 Structure of the phantom for OT.

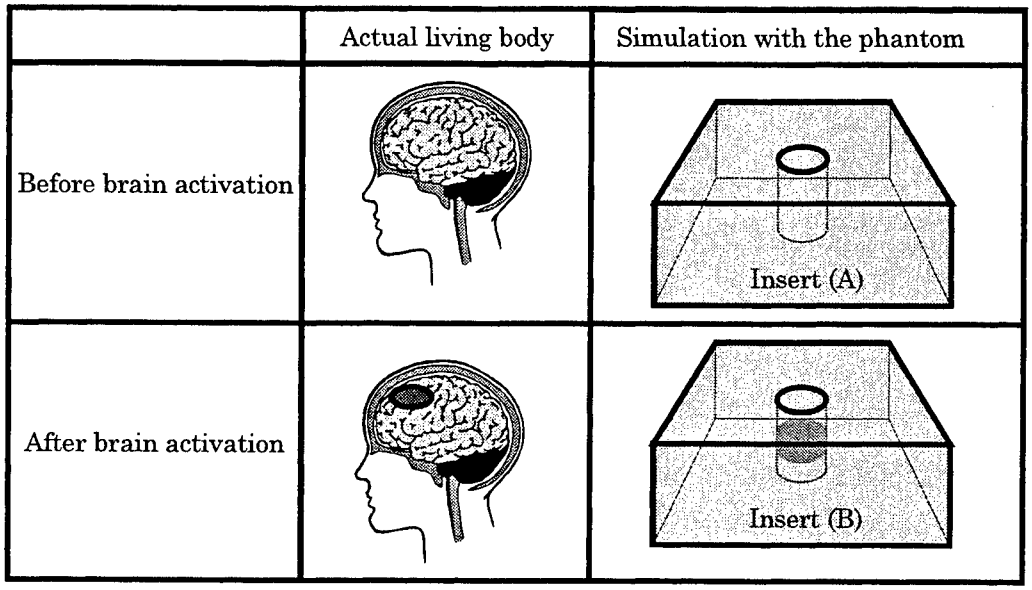

Figure 5 Simulation method of the brain activation in the cortex by the phantom.

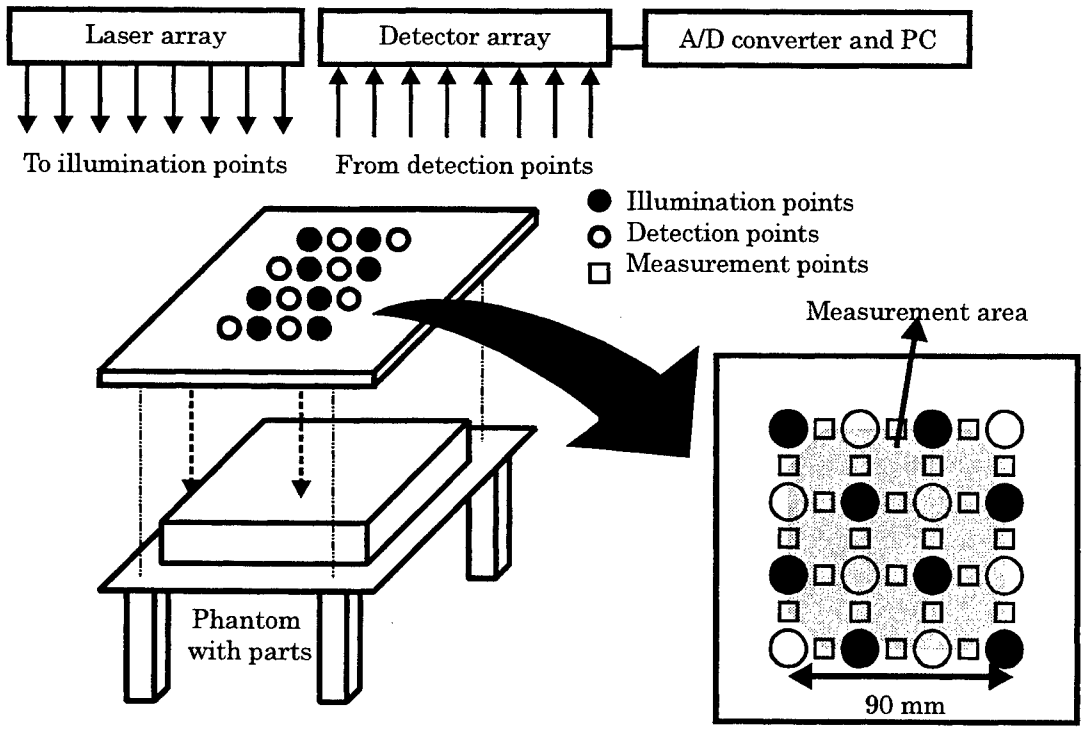

Figure 6 Measurement system to obtain a topographic image of the absorber in the phantom.

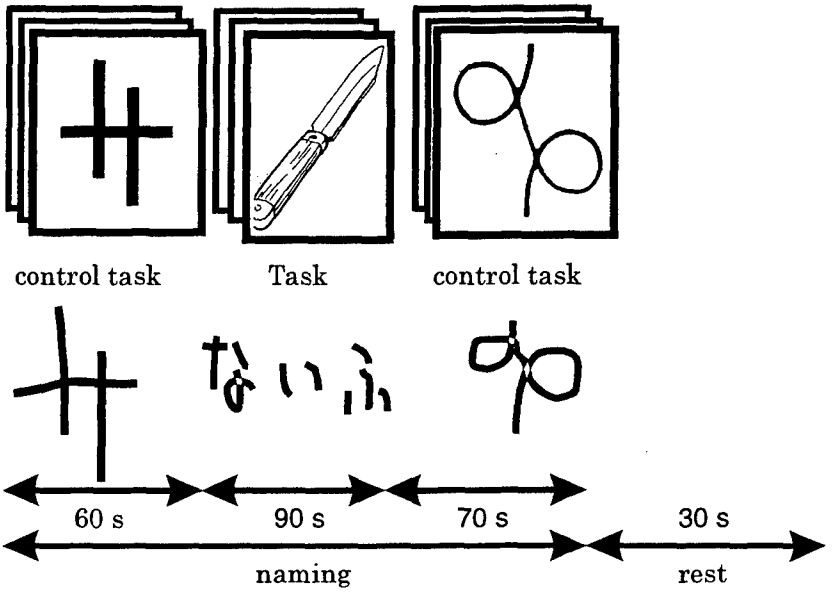

Figure 7 Task sequence for the language function measurement

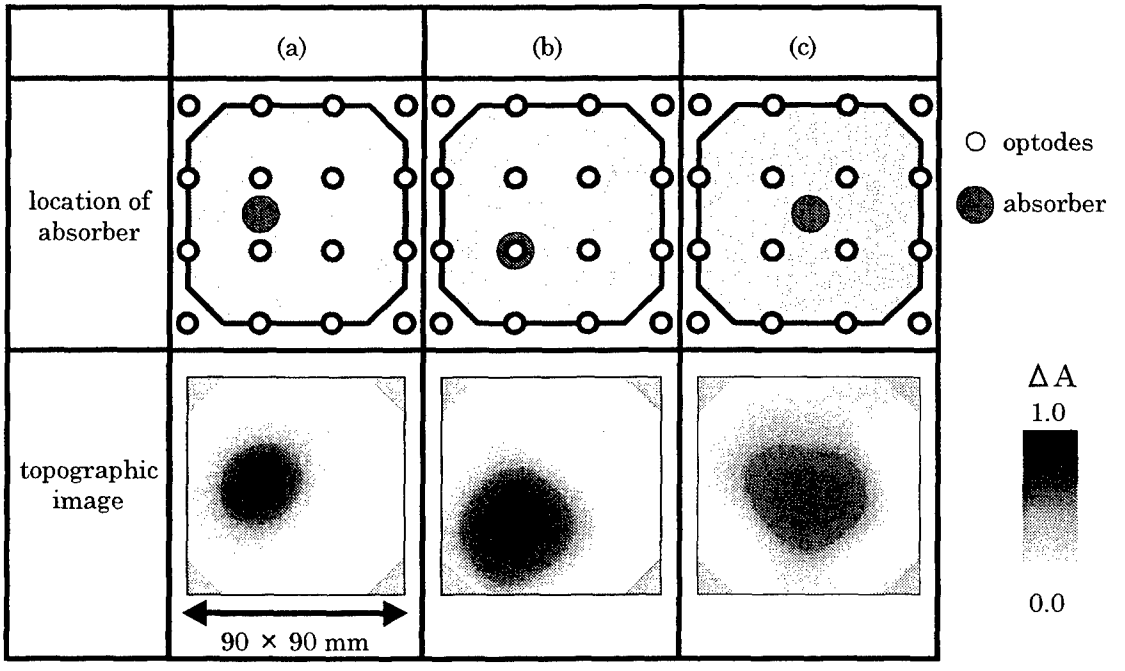

Figure 8 Topographic images of the absorber in the phantom.

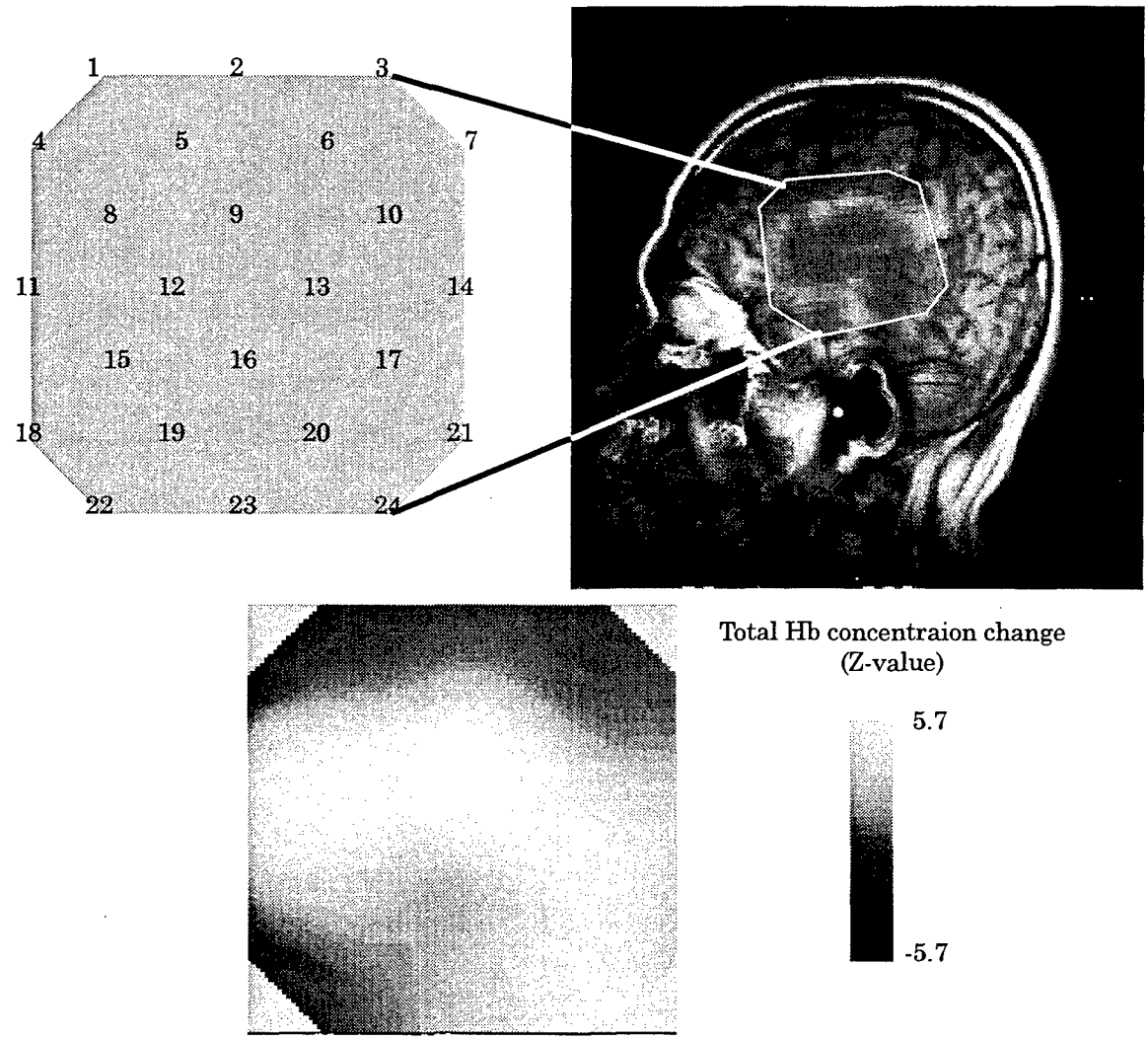

Figure 9 Topographic image (total-Hb concentration change) of the language function and anatomic MRI.

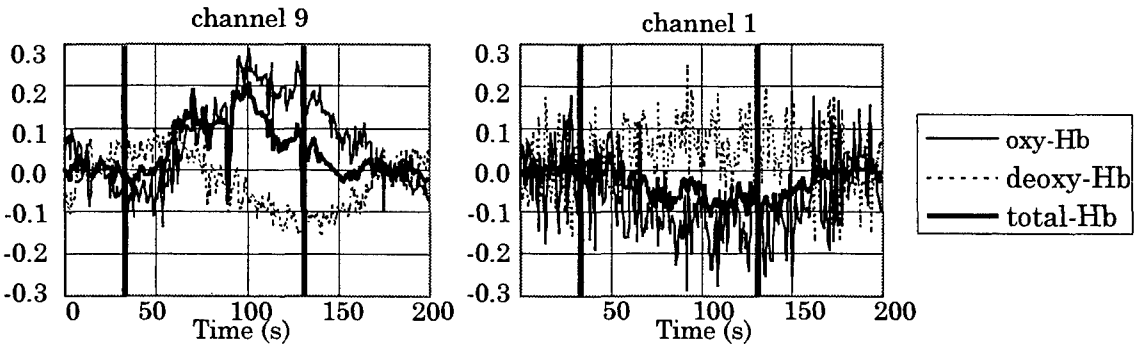

Figure 10 Time responses of the concentration changes (oxy-Hb, deoxy-Hb, and total Hb) for channels 1 and 9 in Fig. 9. The two thick vertical lines in these figures denote the start and the end of the writing task.